

RatGene: Gene deletion-addition algorithms using growth to production ratio for growth-coupled production in constraint-based metabolic networks

Yier Ma^{1,2}, Takeyuki Tamura^{1,2}

¹Bioinformatics Center, Institute for Chemical Research, Kyoto University, Kyoto, Japan

²Graduate School of Informatics, Kyoto University, Kyoto, Japan

Email: mayier@kuicr.kyoto-u.ac.jp, tamura@kuicr.kyoto-u.ac.jp

Abstract

In computational metabolic design, it is often necessary to modify the original constraint-based metabolic networks to lead to growth-coupled production, where cell growth forces target metabolite production. However, in genome-scale models, finding strategies to simultaneously delete and add genes to induce growth-coupled production is challenging. This is particularly true when heavy computation is necessary due to numerous gene deletions and additions. In this study, we mathematically defined related problems, proved NP-hardness and/or NP-completeness, and developed an algorithm named RatGene that (1) automatically integrates multiple constraint-based metabolic networks, (2) identifies gene deletion-addition strategies by a growth-to-production ratio-based approach, and (3) eliminates redundant gene additions and deletions. The results of computational experiments demonstrated that the RatGene-based approach can significantly improve the success ratio for identifying the strategies for growth-coupled production. RatGene can facilitate a more rational approach to computational metabolic design for the production of useful substances using microorganisms by concurrently considering both gene deletions and additions.

Keywords: Biochemistry, Integer linear programming, Constraint optimization

1 Introduction

Computational metabolic design requires adjusting the metabolic functions of microorganisms to create efficient biochemical pathways to produce beneficial substances. By adding or deleting genes, modifying enzymes, or adjusting cellular processes, the production of food, biofuels, large-scale chemicals, pharmaceuticals, and other bioproducts can be enhanced [6, 11, 16]. Understanding the core principles of metabolism and cell activities is critical in this field, and heavily relies on mathematical modeling techniques.

These techniques involve creating mathematical models that depict the behavior of metabolic systems. Such models allow us to simulate and predict how these systems respond under various conditions, such as the creation of a new metabolic pathway or shifts in nutrient availability.

Constraint-based models of metabolic networks are often used in the design of genome-scale metabolic networks for growth-coupled production. This model assumes a balanced metabolism characterized by stable flux distributions and consistent metabolite concentrations. This implies that the total production rates are equal to the total consumption rates for each metabolite. This assumption simplifies the modeling and analysis of metabolic systems, promoting the use of mathematical models to design genome-scale metabolic networks for growth-coupled production. In constraint-based models, reactions are classified into two categories: internal and external reactions. Internal reactions simultaneously produce and consume metabolites, while external reactions either consume or produce metabolites, but not both at the same time. For each reaction rate, lower and upper bounds are provided, with negative values being allowed for reversible reactions.

The **cell growth reaction** and the **target metabolite production reaction** are of particular interest in the constraint-based models. The cell growth reaction is a virtual reaction designed to match the cell growth rate of the biological experiments. It reflects the efficient conversion of absorbed resources into cellular energy and chemical constituents, and the facilitation of cellular evolution under selection pressure [10]. The constraint-based models prioritize maximizing cell growth for this reason. The reaction generating the target metabolite is called the target metabolite production reaction. Such analysis based on the constraint-based models is called flux balance analysis (FBA), which limits biomass production and nutrient availability, as well as focuses on target chemical synthesis. The aim of the FBA-based methods is to investigate and optimize metabolic flux distributions [14].

A common computational task in metabolic engineering is to design constraint-based models for **growth-coupled production**. Let **GR** and **PR** represent the rates of cell growth and target metabolite reactions, respectively. In this study, growth-coupled production is defined as a condition where the minimum values of PR and GR are 0.001 mmol/gDW/h or more when GR is maximized. Metabolic network design is often identified by reaction deletion strategies from the original constraint-based models.

One of the most efficient methods to determine the reaction deletion strategies for growth-coupled production is the elementary mode (EM) and/or minimum cut set (MCS)-based methods, which utilize non-decomposable steady-state fluxes in the design of constraint-based models [1, 22]. The MCS-based method developed by von Kamp et al. demonstrated that growth-coupled production was feasible for almost all metabolites under appropriate conditions in genome-scale metabolic models of five key industrial species [31].

However, reaction deletions are realized by gene deletions because many chemical reactions are catalyzed by enzymes encoded by genes in metabolic networks. Identifying gene deletion strategies for growth-coupled production remains challenging due to intensive computation, especially with complex **gene-protein-reaction (GPR) rules** and

many necessary gene deletions in genome-scale models [9, 19, 27]. In the constraint-based models, GPR rules represent the relationships between genes and reactions with Boolean functions, where the inputs are genes and the outputs are reactions. When a reaction is inhibited due to gene deletions via GPR rules, both the lower and upper bounds of the reaction rate are forced to be zero.

Recently, Tamura et al. developed gDel_minRN by considering GPR rules to identify gene deletion strategies to extract the core part for growth-coupled production [29]. However, the success ratio of gDel_minRN still has room for improvement. Introducing genes from other species is another powerful approach to improve the success ratio. If we can combine multiple constraint-based models and obtain appropriately a larger reference network that contains all potential additions, the modification strategies consisting of gene additions and deletions can be identified through gene deletions from the larger network.

In this study, we developed RatGene, which (1) integrates two constraint-based models N_1 and N_2 , (2) identifies modification strategies, consisting of gene additions and deletions from N_1 , for growth-coupled production, and (3) reduces the size of the modification strategies. In the computational experiments, the performance of RatGene on various datasets was compared with that of existing methods, GDLS and gDel_minRN [7, 29]. The results of the computational experiments showed that (1) for many target metabolites, RatGene can calculate a gene deletion-addition strategy even when gDel_minRN cannot, (2) by using gDel_minRN and RatGene in a complementary manner, gene deletion-addition strategies that lead to growth-coupled production can be calculated for more target metabolites, and (3) RatGene is efficient for identifying gene deletion strategies (without gene addition) as well.

The remaining of this paper is as follows: Section 2.1 briefly summarizes the constraint-based models; Section 2.2 defines problems and proves NP-hard and NP-complete; Section 2.3 explains the workflow of the developed algorithm RatGene; Section 2.4 describes the integration process of two models; Section 2.5 introduces how RatGene determines the initial modification strategies; Section 2.6 states the process to minimize the size of the modification strategies. Then, computational experiments conducted in this study are reported in Section 3: Sections 3.1 and 3.2 are for gene deletion-addition and deletion problems, respectively. Sections 4.1, 4.2, and 4.3 are for discussion, conclusion, and related works, respectively.

2 Method

2.1 Constraint-based Models of Metabolic Networks

A constraint-based model $N = \{R, M, G, S, lb, ub, h\}$ of metabolic networks is composed of a set of **reactions** R , a set of **metabolites** M , a set of **genes** $G = \{g_1, \dots, g_l\}$, a **stoichiometric matrix** S , a set of **lower bounds** of reaction rates lb , a set of **upper bounds** of reaction rates ub , and a set of **GPR** rules h . In the context of constraint-based models of metabolic networks, the important thermodynamic properties of the system are encoded within the stoichiometric matrix S . This matrix is of dimensions $m \times n$, where

m and n represent the number of metabolites and reactions in the network, respectively. A **mode** is a flux vector $v \in \mathbb{R}^n$ in the null space of S , $N(S) = \{v | S \cdot v = 0\}$. This implies that the consumption and production rates of any metabolite in the network are equal in order to maintain the stability of its concentrations:

$$S \cdot v = 0 \quad (1)$$

For accurate representation of the reaction rates of n reactions, the following inequalities must hold true:

$$lb_i \leq v_i \leq ub_i \quad i \in \{1, 2, \dots, n\} \quad (2)$$

This imposes limitations on the lower bound and the upper bound of the reaction rates, respectively, as the magnitude of the reaction rate in the system cannot be infinitely high or low. Furthermore, GPR rules given by Boolean functions are represented as follows:

$$p_i = h_i(G) \quad (3)$$

Each element of G is a binary variable, taking on a value of either 0 or 1. h is a Boolean function that typically has two forms:

$$h_i = \bigwedge_{j=1}^{\lambda_j} \gamma_j, \quad \gamma_j \in \{g, h\} \quad (4)$$

$$h_i = \bigvee_{j=1}^{\lambda_j} \gamma_j, \quad \gamma_j \in \{g, h\} \quad (5)$$

Here, γ is either a gene g or another Boolean function h , and λ is the number of entities in h . These two forms can be represented by the following two linear inequalities:

$$1 - \lambda + \sum \gamma \leq \lambda \cdot h_i \leq \sum \gamma \quad (6)$$

$$\sum \gamma \leq \lambda \cdot h_i \leq \lambda \cdot \sum \gamma \quad (7)$$

The inequalities (2) then can be modified as:

$$p_i \cdot lb_i \leq v_i \leq p_i \cdot ub_i, \quad (8)$$

where p_i indicates whether the reaction v_i is deleted. In FBA, the vector space V is defined by inequalities (1) to (8). This vector space represents the feasible solution space. Within this space, the objective is to find an optimal solution that satisfies the objective function of the mixed integer linear programming (MILP) problem P :

$$\max \quad f(v) \quad (9)$$

s.t.

$$S \cdot v = 0$$

$$p_i \cdot lb_i \leq v_i \leq p_i \cdot ub_i$$

$$p_i = h_i(g),$$

where $f(v)$ is the objective function. The problem for maximizing $f(v)$ on the vector space V is denoted by $P_V^{f(v)}$. When $f(v)$ is GR, the problem is denoted as $P_V^{v_{growth}}$, where the cell growth reaction rate v_{growth} is maximized. The solution $x_V^{f(v)}$ represents a vector that indicates the rates of n reactions when maximizing $f(v)$ in V . We need to identify a subspace $U \subseteq V$ such that the solution $x_U^{f(v)}$ of the problem $P_U^{f(v)}$ satisfies $GR \geq 0.001$ and $PR \geq 0.001$. The subspace U represents a space induced by a modification strategy, specifically a deletion strategy in this case. The modification strategy D is a 0/1 assignment for each gene, which represents either deletion or retention of the associated gene. Any space derived from a specific D is a subspace of the original vector space V .

For example, consider a constraint-based model where $l = 3$, $n = 2$, and the GPR rules are given by $p_1 = g_1 \wedge g_2$ and $p_2 = g_1 \vee g_3$. Let us consider a modification strategy $D_e = (1, 0, 0)$, which implies $g_1 = 1$, $g_2 = 0$, and $g_3 = 0$. The following illustrate the original feasible solution space V_e and the subspace U_e derived from the modification strategy D_e , where genes g_2 and g_3 are deleted.

V_e	U_e
$S \cdot v = 0$	$S \cdot v = 0$
$p_1 \cdot lb_1 \leq v_1 \leq p_1 \cdot ub_1$	$v_1 = 0$
$p_2 \cdot lb_2 \leq v_2 \leq p_2 \cdot ub_2$	$lb_2 \leq v_2 \leq ub_2$
$p_1 = g_1 \wedge g_2$	$p_1 = 0$
$p_2 = g_1 \vee g_3$	$p_2 = 1$

Figure 1(A) provides a toy example network to describe the assumption of the flux balance and the growth-coupled production. This simple example network contains seven reactions $\{R1, R2, R3, R4, R5, R6, R7\}$ and three metabolites $\{C1, C2, C3\}$, where R1 is the input to the network and R6 and R7 are the outputs of the network. R6 and R7 are the cell growth and the target metabolite production reactions, respectively. The upper and lower bounds of all reactions are attached as $[\epsilon_x, \epsilon_y]$ in the figure. Figure 1(B) illustrates the stoichiometric matrix S corresponding to this example network. Each row represents the relationship between a metabolite and all reactions, and each entry indicates the coefficient by which that metabolite is produced or consumed per occurrence of that reaction. For example, the first row indicates that C1 is generated by R1 but consumed by R2, R3, and R4. The assumption of flux balance means that the concentration of any metabolite is stable. For instance, the inner product of the first row of S and a flux vector $[2, 1, 1, 0, 0, 0, 0]^T$ ensures the change of the concentration of C1 is 0. One of the valid flux vectors for the wild type is given by $[2, 2, 0, 0, 0, 2, 0]^T$. Since the flux of R2 can be substituted with R3 and R5, for example, the vector $[2, 0, 2, 0, 2, 2, 0]^T$ is also valid.

Figure 1(C) is a table representing deletion strategies and the resulting flux rates. The deletion strategy $\{R3, R5\}$ induces the flux vector $[2, 0, 0, 2, 0, 2, 2]^T$ in the optimistic scenario (best-case) regarding R7. This is the state of growth-coupled production since the target metabolite production reaction rate is not zero when the growth reaction is maximized under the assumption of flux balance. However, this deletion

strategy would not ensure a constant growth-coupled production because the flux vector $[2, 2, 0, 0, 0, 2, 0]^T$ is obtained in the pessimistic scenario (worst-case) regarding R7. To ensure growth-coupled production even in the worst-case scenario for the target metabolite production, we should delete $\{R2, R5\}$. And this deletion strategy induces the flux vector $[2, 0, 0, 2, 0, 2, 2]^T$, which ensures the growth-coupled production even in the worst case.

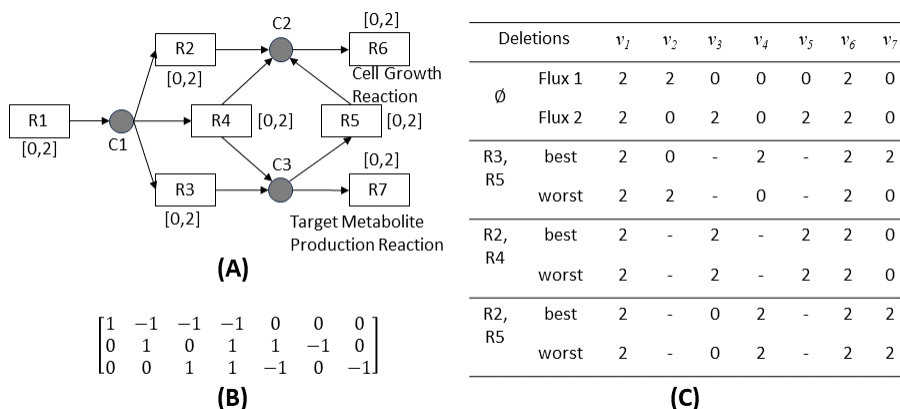


Figure 1. (A) An example network. (B) The stoichiometric matrix. (C) A table represents deletion strategies and flux rates.

2.2 Problem Definition

We consider four types of problems for finding $x_U^{f(v)}$ in $P_U^{f(v)}$. The gene deletion problem for maximizing the minimum v_{target} is defined as follows, where v_{target} is the target metabolite production reaction.

Problem 1 Find D that derives the subspace U of the original vector space V , subject to $U = \operatorname{argmax}_{U \subseteq V} (\min v_{target})$ in $P_V^{v_{growth}}$.

Instead of maximizing the minimum PR with GR maximization, its decision problem version is defined with the thresholds $lb_{target}^{threshold}$ and $lb_{growth}^{threshold}$ for v_{target} and v_{growth} .

Problem 2 (Prob-gDel): Find D that derives the subspace U of the original vector space V , subject to $v_{target} \geq lb_{target}^{threshold}$ and $v_{growth} \geq lb_{growth}^{threshold}$ for any v_{target} in $P_V^{v_{growth}}$. "No solution" is returned if there is no such D .

When $lb_{target}^{threshold}$ gradually increases, Problem 2 approaches to Problem 1.

Theorem 1 Problem 1 is NP-hard.

Proof. The NP-hardness is proved by the reduction from the 3-SAT problem [23]. Any instance of the 3-SAT problem can be represented by the constraint-based models as shown in Figure 2. The rectangles and circles with solid borders are reactions and metabolites, respectively. All coefficients related to reactions are set to 1 unless otherwise specified. Figure 2(A) shows the representation of a literal. g_i is a gene that controls the reaction x_k : $g_i = 1$ makes x_k active while $g_i = 0$ makes x_k inactive. Suppose that $g_i = 1$ holds. Since $\bar{x}_i = x_k = 1$ always holds, all flow from \bar{x}_i reaches x_k , but not to \bar{x}_j . All flow from x_i reaches x_j , but not to \bar{x}_j . Then, $x_j = 1$ and $\bar{x}_j = 0$ hold. Next, Suppose that $g_i = 0$ holds. Because $x_k = 0$ and $\bar{x}_i = 1$ must hold, all flow from \bar{x}_i must be consumed by \bar{x}_j . The flow from x_i is consumed by \bar{x}_j and cannot reach x_j . Then, $x_j = 0$ and $\bar{x}_j = 1$ hold. Thus, The network of Figure 2(A) ensures that l_i is produced from x_j when $g_i = 1$ and from \bar{x}_j when $g_i = 0$.

Figure 2(B) shows the representation of a clause of the 3-SAT instance. The rectangles with dashed borders are networks of literals shown in (A). The metabolite u is produced by x_j for a positive literal of the original 3-SAT while by \bar{x}_j for a negative literal in Figure 2(A). C_m represents a reaction $u \rightarrow y$, C_p represents a reaction $2 \cdot u \rightarrow y$, and C_n represents a reaction $3 \cdot u \rightarrow y$. This ensures the existence of the case that one y is produced when at least one literal is true. Specifically, C_m , C_p , or C_n is used depending on whether the number of satisfied literals is 1, 2, or 3, respectively.

Using the sub-networks illustrated in Figure 2(A) and (B), any 3-SAT problem can be represented by the constraint-based model of Figure 2(C). Rectangles with dashed borders are clauses formed by (B). PR and GR are the target metabolite production and the cell growth reactions, respectively. Growth-coupled production, defined by $x_{growth} \geq 0.001$ and $x_{target} \geq 0.001$ hold for any $x_{target} \in x_U^{v_{growth}}$, is achieved only when $GC = GR = PR = 1$ holds. Since l_i , l_j , and l_k are always 1, growth-coupled production is achieved if and only if every y is 1. Therefore, finding a solution for the 3-SAT problem is equal to finding a gene deletion strategy in the constraint-based model. Because this constraint-based model can be obtained from any 3-SAT problem in polynomial time, the original problem is NP-hard. \square

The only distinction between Problems 1 and 2 is that the former is an optimization-based problem while the latter is a decision-based problem. Consequently, the following lemma can be derived.

Lemma 1 *Problem 2 is NP-complete.*

Proof. Problem 2 is NP-hard even when $lb_{growth}^{threshold}$ and $lb_{target}^{threshold}$ are limited to 1 according to the proof in Theorem 1. Because any solution can be verified in polynomial time, Problem 2 is in NP. Since Problem 2 is in NP and NP-hard, the NP-completeness is proved. \square

Problems 1 and 2 focus on deletion strategies. However, in the following, we extend the problem definitions to simultaneously consider both deletion-addition strategies.

We consider a larger constrain-based model $N_I = \{R_I, M_I, G_I, S_I, lb_I, ub_I, h_I\}$ in addition to the original $N = \{R, M, G, S, lb, ub, h\}$, where $R \subseteq R_I$, $M \subseteq M_I$, and

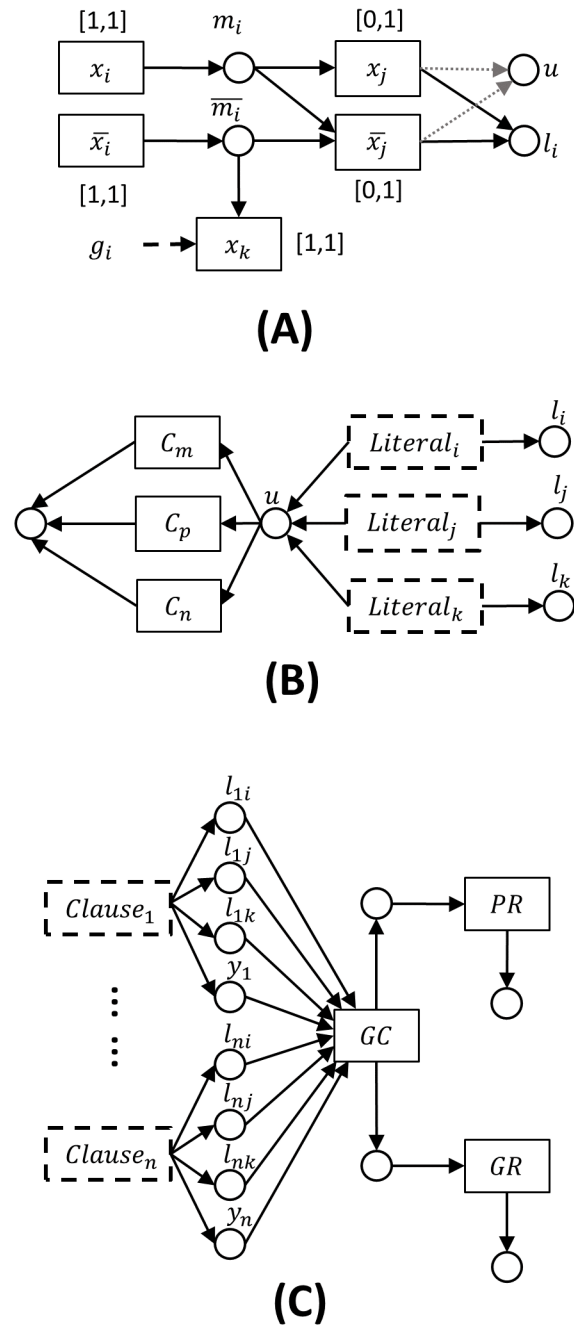


Figure 2. How to convert a 3-SAT problem into the gene deletion problem in a constraint-based model. (A) A network representing a literal. (B) A network representing a clause. (C) A network representing a 3-SAT problem.

$G \subseteq G_I$ hold. Let V_I and V be the vector spaces for N_I and N , respectively. In the extended problem, a deletion strategy D_I induces a subspace U_I of V_I . U_I consists of a subspace U of V and an additional space U' , which is a subspace of $N_I - N$. This additional space U' consists of additional n' reactions, m' metabolites, and l' genes. The union $U \cup U'$ needs to simultaneously satisfy the constraints (1) to (8).

Then, Problem 1 is converted to as follows.

Problem 3 Find D_I that derives the subspace $U_I = U \cup U'$ of V_I , subject to $U_I = \operatorname{argmax}_{U \subseteq V, U' \not\subseteq V} (\min v_{target})$ in $P_{V_I}^{v_{growth}}$.

Similarly, we can define the decision version of Problem 3.

Problem 4 (Prob-gDel-Add): Find D_I that derives the subspace $U_I = U \cup U'$ of V_I , subject to $v_{growth} \geq lb_{growth}^{threshold}$ and $v_{target} \geq lb_{target}^{threshold}$ for any v_{target} in $P_{V_I}^{v_{growth}}$. "No solution" is returned if there is no such D_I .

The following lemma is held for Problems 3 and 4.

Lemma 2 Problem 3 is NP-hard, and Problem 4 is NP-complete.

Proof. When $N_I = N$, Problems 3 and 4 are equivalent to Problems 1 and 2, respectively. Therefore, Problems 3 and 4 are NP-hard. Since we can validate D_I in polynomial time for Problem 4, it is in NP. Since Problem 4 is NP-hard and in NP, it is NP-complete. \square

2.3 Workflow of RatGene

Algorithm 0 describes the workflow of RatGene, which integrates two constraint-based models N_c and N_e by Algorithm 1, determines a modification strategy for growth-coupled production by Algorithm 2, and reduces the strategy size by Algorithm 3. Algorithm 3 calls Functions 1 and 2 for the reduction of gene deletions and additions, respectively. Algorithms 1 to 3 and Functions 1 and 2 are described in the following subsections.

Algorithm 0 RatGene

Input: constraint-based model N_c and N_e , target metabolite

Output: A modification strategy D_{min} for growth-coupled production

- 1: **if** $N_e \notin \emptyset$ **then**
 - 2: model integration of N_c and N_e to obtain N_i by Algorithm 1
 - 3: **end if**
 - 4: obtain the modification strategy D by Algorithm 2
 - 5: obtain D_{min} by Algorithm 3
-

2.4 Model Integration

Problems 2 (Prob-gDel) and 4 (Prob-gDel-Add) described in Section 2.2 are the main problems in this study. Prob-gDel-Add is the same as Prob-gDel after integrating two constraint-based models. For the integration of two constraint-based models, a **core model** $N_c = \{R_c, M_c, G_c, S_c, lb_c, ub_c, h_c\}$ is selected first, and then the other is defined as the **edge model** $N_e = \{R_e, M_e, G_e, S_e, lb_e, ub_e, h_e\}$. Reactions included in the edge model but not in the core model are defined as $R_{ec} = R_e \setminus \{R_e \cap R_c\}$; their lower and upper bounds and GPR rules are represented by lb_{ec} , ub_{ec} , and h_{ec} , respectively. Metabolites and genes associated with R_{ec} are represented by M_{ec} and G_{ec} , respectively. Then, additional reactions R_{ec} , metabolites $M^{ec} = M_{ec} \setminus \{M_{ec} \cap M_c\}$ and genes $G^{ec} = G_{ec} \setminus \{G_{ec} \cap G_c\}$ are added to the core model to form the integrated model: $N_I = \{R_I = R_{ec} \cup R_c, M_I = M^{ec} \cup M_c, G_I = G^{ec} \cup G_c, lb_I = lb_{ec} \cup lb_c, ub_I = ub_{ec} \cup ub_c, h_I = h_{ec} \cup h_c\}$. The integrated stoichiometric matrix S_I is constructed by a horizontal concatenation of two matrices as shown in Figure 3. The left-part matrix is formed by a vertical concatenation of a zero matrix with $|M^{ec}|$ rows and $|R_c|$ columns below the matrix S_c . And the right-part matrix is made by a vertical concatenation of a zero matrix and the matrix S_{ec} , which corresponds to metabolites M_{ec} and reactions R_{ec} with $|M_{ec}|$ rows and $|R_{ec}|$ columns. This results in the integrated model $N_I = \{R_I, M_I, G_I, S_I, lb_I, ub_I, h_I\}$ retain the same format as the core model. Algorithm 1 is the pseudo-code for the model integration.

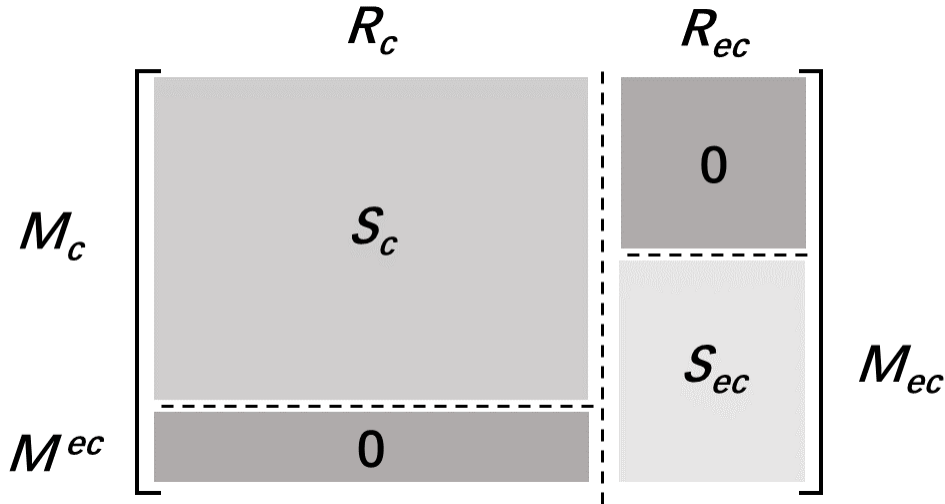


Figure 3. The structure of the integrated stoichiometric matrix S_I .

For example, Figures 4(A) and 4(B) represent a core and an edge model, respectively. Figure 4(C) is the integrated model consisting of the core model and a part of the edge model. R_c and R_{ec} are $\{R1,R2,R3,R6,R7,R8,R9,R10,R11\}$ and $\{R4,R5\}$, respectively. According to the definition, M_c , M_{ec} , and M^{ec} are then $\{C1,C2,C3,C5,C6,C7\}$, $\{C1,C3,C4,C6\}$, and $\{C4\}$, respectively. Thus, S_c is the stoichiometric matrix of the core model and S_{ec} is a part of the stoichiometric matrix of the edge model. And this S_{ec} is a matrix with a size of four rows and two columns, which is specifically composed with

Algorithm 1 Model Integration

Input: core model N_c , edge model N_e
Output: integrated model $N_I = \{R_I, M_I, G_I, S_I, lb_I, ub_I, h_I\}$

```

1:  $R_{ec} \leftarrow R_e \setminus \{R_e \cap R_c\}$ 
2: obtain  $M_{ec}, G_{ec}, h_{ec}, lb_{ec}$ , and  $ub_{ec}$  corresponding to  $R_{ec}$ 
3:  $R_I = R_{ec} \cup R_c, lb_I = lb_c \cup lb_{ec}, ub_I = ub_c \cup ub_{ec}, h_I = h_c \cup h_{ec}$ 
4:  $M^{ec} \leftarrow M_{ec} \setminus \{M_{ec} \cap M_c\}, G^{ec} \leftarrow G_{ec} \setminus \{G_{ec} \cap G_c\}$ 
5:  $M_I \leftarrow M^{ec} \cup M_c, G_I \leftarrow G^{ec} \cup G_c$ 
6:  $S_{II} \leftarrow [S_c; zeros(|M^{ec}|, |R_c|)]$  //vertical concatenation
7: for  $i = 1$  to  $|M_I|$  do
8:   if  $M_I(i) \in M_{ec}$  then
9:      $S_{Ir}[i][:] \leftarrow S_e[position(M_I(i) \text{ in } M_e)][:]$ 
10:  else
11:     $S_{Ir}[i][:] \leftarrow 0$ 
12:  end if
13: end for
14:  $S_I \leftarrow [S_{II}|S_{Ir}]$  //horizontal concatenation

```

the interaction of rows corresponding to $\{C1, C3, C4, C6\}$ and columns corresponding to $\{R4, R5\}$ from the original stoichiometric matrix S_e in the edge model.

2.5 Strategy Generation

In the next phase of RatGene, a ratio-based constraint is iteratively applied to systematically construct MILP problems. These problems can then be used to determine a modification strategy. In each iteration of the loops, a different ratio-based MILP problem is formulated and solved. Each MILP problem ensures the flux balance assumption and sets the upper and lower bounds of the reaction rates. Due to the need to simulate the functioning of biological systems, certain specific reactions have assigned thresholds for their lower and/or upper bounds. Typically, thresholds are set to both the minimum rate for cell growth reactions and the maximum rates for oxygen and glucose uptake reactions. These reactions are crucial for the survival and functioning of microorganisms:

$$v_{biomass} \geq lb_{biomass}^{min} \quad (10)$$

$$v_{oxygenUptake} \leq ub_{oxygenUptake}^{max} \quad (11)$$

$$v_{glucoseUptake} \leq ub_{glucoseUptake}^{max} \quad (12)$$

The associations between GPR rules and their corresponding reactions can be represented by linear constraints [29].

A predetermined value α restricts the ratio between the target reaction rate v_{target} and the growth reaction rate $v_{biomass}$. However, the appropriate value of α is unknown and different for different networks and different target metabolite production reactions. Therefore, loops are designed to iteratively assign different constants to find an appropriate value for α .

According to the ratio constraint $v_{target} \cdot v_{biomass}^{-1} = \alpha$, clearly, $\alpha \in [0 \cdot TMGR^{-1}, TMPR \cdot lb_{biomass}^{min}^{-1}]$ can be obtained because the values of v_{target} and $v_{biomass}$ are both non-negative and the lb for $v_{biomass}$ should be greater than zero by the problem definition, where $TMPR$ is the theoretical maximum production rate and $TMGR$ is the theoretical maximum growth rate. A constant value $TMPR \cdot lb_{biomass}^{min}^{-1} \cdot maxLoop^{-1} \cdot loop$ is added to the value of α in each iteration of the loops. Here, $maxLoop$ is the total number of iterations and $loop$ is the cumulative number of iterations. The objective function of each MILP problem is constructed as minimizing the sum of l_0 -Norm of the reactions scaled by $TMGR$ and the negative value of the cell growth reaction rate. Then, the MILP problem is formulated as (13). Figure 4 shows an example of the importance of the extra ratio constraint and the reason why such an objective function is designed.

$$\begin{aligned}
 \min \quad & -v_{biomass} + TMGR \cdot \|v_Q\|_0 \tag{13} \\
 \text{s.t.} \quad & \\
 & S \cdot v = 0 \\
 & p_i \cdot lb_i \leq v_i \leq p_i \cdot ub_i \\
 & p_i = h_i(g) \\
 & v_{biomass} \geq lb_{biomass}^{min} \\
 & v_{oxygenUptake} \leq ub_{oxygenUptake}^{max} \\
 & v_{glucoseUptake} \leq ub_{glucoseUptake}^{max} \\
 & \frac{v_{target}}{v_{biomass}} = \alpha \\
 & 0 \leq \alpha \leq \frac{TMPR}{lb_{biomass}^{min}} \\
 & Q = \{q \mid \exists h_q\}
 \end{aligned}$$

For example, for a core and an edge model as shown in Figures 4(A) and 4(B), the integrated model is obtained as shown in Figure 4(C). The edge model shares the same internal reaction R6 with the core model. The input is reaction R1 which plays a role of the nutrient uptake reaction, and the outputs are reactions R10 and R11, where R10 is the cell growth reaction and R11 is the target metabolite production reaction.

In Figure 4(C), $\{R1, R2, R3, R10\}$, $\{R1, R7, R8, R11\}$, $\{R1, R6, R7, R8, R9\}$, $\{R1, R4, R5, R10, R11\}$, and $\{R1, R4, R5, R6, R9, R10\}$ are the five elementary modes whose linear combinations satisfy the constraint 1. Among these elementary modes, $\{R1, R4, R5, R10, R11\}$ is included in neither the core model nor the edge model, so it is the newly generated elementary mode as a result of the integration of two models. To achieve the growth-coupled production, $\{R1, R4, R5, R10, R11\}$ can be the choice under the condition that the ratio between R10 and R11 is determined to be 1 and this could even satisfy the criterion for the worst-case analysis. However, a linear combination of $\{R1, R2, R3, R10\}$ and $\{R1, R7, R8, R11\}$ is also possible to make the ratio fixed at 1 in Figure 4(C). The number of reactions required by the linear combination of $\{R1, R2, R3, R10\}$ and $\{R1, R8, R9, R11\}$ is seven which is greater than the number of

reactions for $\{R1, R4, R5, R10, R11\}$. Therefore, minimizing l_0 -Norm of the reactions and imposing $\alpha = 1$ results in finding an effective reaction deletion strategy for this example. When multiple solutions exist in minimizing l_0 -Norm, GR is maximized. To this end, $TMGR$ is multiplied by the l_0 -Norm to reflect the priority in the objective function. The feasible solution is deleting reactions $\{R2, R3, R6, R7, R8, R9\}$ in the integrated model, Figure 4 (C), that is, deleting $\{R2, R3, R6, R7, R8, R9\}$ and adding $\{R4, R5\}$ to the core model, Figure 4 (A).

To obtain the modification strategies at the gene level, only reactions with GPR rules are considered for the l_0 -Norms. The modification strategy can be represented by deleting $\{g1, g2, g3, g4, g6, g7\}$ in the integrated model, that is, deleting $\{g1, g2, g3, g4, g6, g7\}$ and adding $\{g8, g9\}$ in the core model. It is to be noted that the modification strategy at the gene level does not always exist for a designated reaction deletion strategy. In RatGene, the modification strategy at the gene level is directly determined by MILP.

The obtained modification strategy consists of six gene deletions and two gene additions for the core model. The reduced modification strategy by the process described in Section 2.6 consists of five gene deletions $\{g1, g2, g4, g6, g7\}$ and two gene additions $\{g8, g9\}$. Algorithm 2 summarizes the process of strategy generation.

Algorithm 2 Strategy Generation

Input: constraint-based model N , v_{target} , $maxLoop$, $TMGR$

Output: D

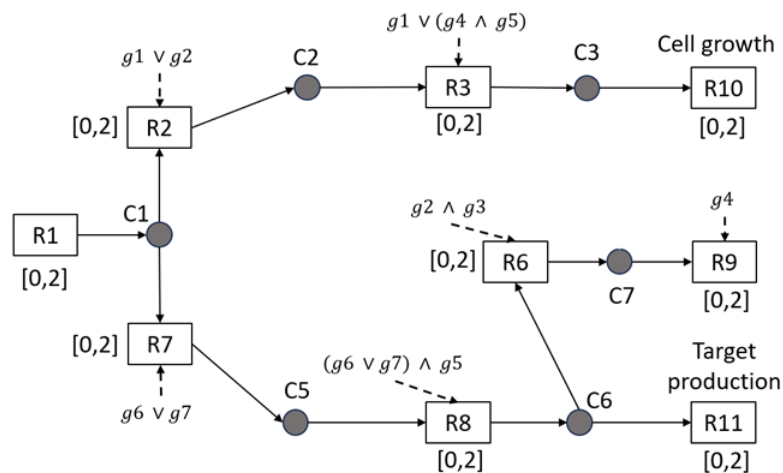
```

1: Initialization:  $\alpha \leftarrow 0$ ,  $loop \leftarrow 1$ 
2: Form problem  $P_V^{v_{target}}$ ,  $V$  derives from (1) to (5)
3:  $TMPR \leftarrow lp(P_V^{v_{target}})$ 
4:  $gap \leftarrow \frac{TMPR}{lb_{biomass}^{min} \cdot maxLoop}$ 
5: if  $TMPR > 10^{-3}$  then
6:   Form problem  $P_{V^{(13)}}^{f^{(13)}}$  based on (13)
7:   while  $loop \leq maxLoop$  do
8:      $\alpha \leftarrow \alpha + gap$  //Update  $\alpha$  to (13)
9:      $pool \leftarrow milp(P_{V^{(13)}}^{f^{(13)}})$ 
10:     $D \leftarrow verify(pool)$ 
11:    if  $D \neq \emptyset$  then
12:      return
13:    end if
14:     $loop \leftarrow loop + 1$ 
15:  end while
16: end if

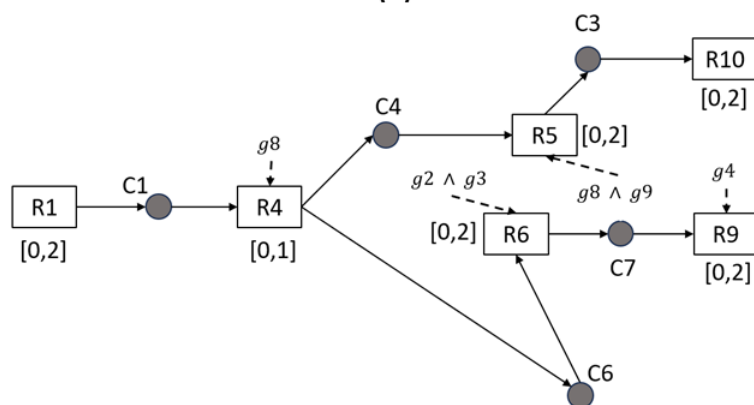
```

2.6 Strategy Size Reduction

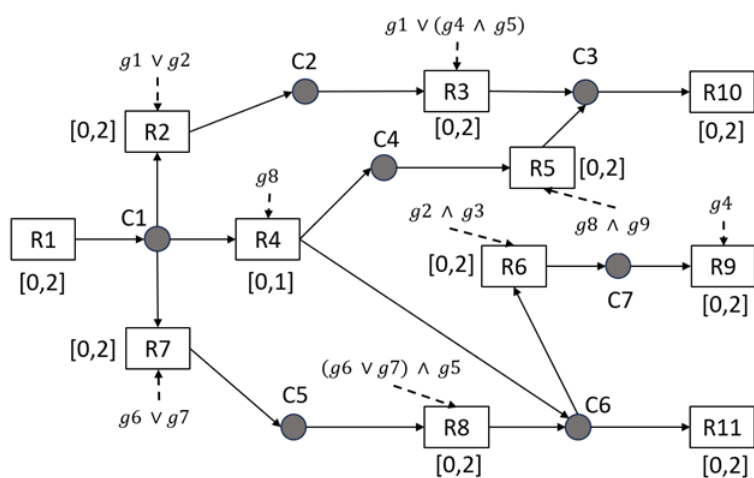
Algorithm 3 reduces the sizes of the modification strategy D consisting of deletion D_d and addition D_a . Algorithm 3 employs Functions 1 and 2 as submodules and its pseudo-code is described below.



(A)



(B)



(C)

Figure 4. A Toy Constraint-based model. R1 to R11, C1 to C7, and $g1$ to $g9$ are reactions, metabolites, and genes, respectively. Bounds and GPR rules are shown as well. (A) The core model. (B) The edge model. (C) The integrated model of the core model and the edge model.

Algorithm 3 Size Reduction for a Modification Strategy

Input: the modification strategy D , $h(g)$

Output: D_{min}

```

1:  $D = D_a \cup D_d$  //divide  $D$  into addition and deletion
2: for  $i = 1$  to  $n$  do //deletion strategy
3:   if  $h_i(D_d) == 0$  then
4:      $\mathbf{D}^i = MinDel(h_i(g), D_d)$  //Function 1
5:   end if
6: end for
7: for  $j = 1$  to  $n$  do //addition strategy
8:   if  $h_j(D_a) == 1$  then
9:      $\mathbf{A}^j = MinAdd(h_j(g), D_a)$  //Function 2
10:  end if
11: end for
12:  $D_{min} = \min \sum g$ 
13:   s.t.  $r_i = \bigvee (\mathbf{conjunction}(\mathbf{D}^i)), i = 1, \dots, n_d$ 
14:        $r_j = \bigvee (\mathbf{conjunction}(\mathbf{A}^j)), j = 1, \dots, n_a$ 
15:        $g = \{0, 1\}$  // 1 indicates deletion in  $\mathbf{D}$  and addition in  $\mathbf{A}$ .
16:        $r_i, r_j = 1$ 

```

Function 1 reduces the size of deletions D_d by considering each reaction forced to be 0 by GPR rules in the core model. The GPR rule $h_i(g)$ associated to the reaction v_i in a constraint-based model can be categorized into three groups based on its formula:

$$\begin{aligned}
 (1) h_i(g) &= \bigwedge_{t=1}^T C_t \\
 (2) h_i(g) &= \bigvee_{t=1}^T C_t \\
 (3) h_i(g) &= g_k.
 \end{aligned}$$

C_t denotes a clause, which can be classified into one of the three types described above. T is the number of clauses. Suppose that $h_i(g)$ is Type (1). For each clause C_t for v_i , if the clause is a gene g_i , that is Type (3), then g_k is added to the deletion list D_z . If a clause is either Type (1) or (2), Function 1 is recursively called. Since Function 1 may return multiple D_z , denoted by \mathbf{D} , the deletion lists are updated by the direct product operation. Next, suppose that $h_i(g)$ is Type (2). Function 1 is recursively called for each clause and len represents the minimum size of deletions in $MinDel(C_t, D_d)$. It is to be noted that multiple clauses have the size len . For such clauses, Function 1 is recursively called and the deletion list \mathbf{D} is updated by the direct product of \mathbf{D} and the result of Function 1. Finally, suppose that $h_i(g)$ consists of a single gene g_k , that is Type (3). Then, g_k is added to \mathbf{D} . Function 1 returns \mathbf{D} as the deletion list with the reduced size.

Similarly, Function 2 reduces the size of additions D_a by considering reactions forced to be 1 by GPR rules outside the core model. Suppose that $h_i(g)$ is Type (1). If a clause

Function 1 Size Reduction for Gene Deletions

```

1: function MINDEL( $h_i(g)$ ,  $D_d$ )
2:    $\mathbf{D} = D_1 \leftarrow \emptyset$ 
3:   if  $h_i(g) = \bigvee_{t=1}^T C_t$  then
4:     for  $C_1$  to  $C_T$  do
5:       if clause  $C_t$  has a single literal  $g_k$  and  $g_k \in D_d$  then
6:          $D_z = D_z \cup g_k$  for all  $z$ 
7:       else if clause  $C_t$  has multiple literals then
8:          $\mathbf{D} = \mathbf{D} \times \text{MinDel}(C_t, D_d)$  /* $\times$  means direct product.
9:       end if
10:    end for
11:   else if  $h_i(g) = \bigwedge_{t=1}^T C_t$  then
12:      $len \leftarrow \min\{\|\text{MinDel}(C_1, D_d)\|, \dots, \|\text{MinDel}(C_T, D_d)\|\}$  /* $len > 0$ 
13:     for  $C_1$  to  $C_T$  do
14:       if  $\|\text{MinDel}(C_t, D_d)\| == len$  then
15:          $\mathbf{D} = \mathbf{D} \times \text{MinDel}(C_t, D_d)$ 
16:       end if
17:     end for
18:   else if  $h_i(g) = g_k$  and  $g_k \in D_d$  then
19:      $\mathbf{D} = g_k$ 
20:   end if
21:   return  $\mathbf{D}$ 
22: end function

```

C_t consists of a single gene g_k , that is Type (3), then g_k is added to the addition list A_z . If a clause is either Type (1) or (2), Function 2 is recursively called. Since Function 2 may return multiple A_z , denoted by \mathbf{A} , the addition lists are updated by the direct product operation. Next, suppose that $h_i(g)$ is Type (2). Function 2 is recursively called for each clause and len represents the minimum size of additions in $\text{MinAdd}(C_t, D_d)$. It is to be noted that multiple clauses have the size len . For such clauses, Function 2 is recursively called and the addition list \mathbf{A} is updated by the direct product of \mathbf{A} and the result of Function 2. Finally, suppose that $h_i(g)$ consists of a single gene g_k , that is Type (3). Then, g_k is added to \mathbf{A} . Function 2 returns \mathbf{A} as the addition list with the reduced size.

Finally, Algorithm 3 conducts integer linear programming (ILP) to obtain the modification strategy with the minimum size using the constraints obtained by Functions 1 and 2.

3 Computational Experiments

All the procedures executed in the computational experiments in this study were implemented on a Ubuntu 20.04 machine with an AMD Ryzen Threadripper3 3970X CPU of 3.70GHz 32C/64T. The running environment is based on IBM ILOG CPLEX 12.10, COBRA Toolbox 2022 and MATLAB R2019b. An auxiliary exchange reaction

Function 2 Size Reduction for Gene Additions

```

1: function MINADD( $h_i(g)$ ,  $D_a$ )
2:    $\mathbf{A} = A_1 \leftarrow \emptyset$ 
3:   if  $h_i(g) = \bigwedge_{t=1}^T C_t$  then
4:     for  $C_1$  to  $C_T$  do
5:       if clause  $C_t$  has a single literal  $g_k$  and  $g_k \in D_a$  then
6:          $A_z = A_z \cup g_k$  for all  $z$ 
7:       else if clause  $C_t$  has multiple literals then
8:          $\mathbf{A} = \mathbf{A} \times \text{MinAdd}(C_t, D_a)$ 
9:       end if
10:    end for
11:  else if  $h_i(g) = \bigvee_{t=1}^T C_t$  then
12:     $len \leftarrow \min\{\|\text{MinAdd}(C_1, D_a)\|, \dots, \|\text{MinAdd}(C_T, D_a)\|\}$  //  $len > 0$ 
13:    for  $C_1$  to  $C_T$  do
14:      if  $\|\text{MinAdd}(C_t, D_a)\| == len$  then
15:         $\mathbf{A} = \mathbf{A} \times \text{MinAdd}(C_t, D_a)$ 
16:      end if
17:    end for
18:  else if  $h_i(g) = g_k$  and  $g_k \in D_a$  then
19:     $\mathbf{A} = g_k$ 
20:  end if
21:  return  $\mathbf{A}$ 
22: end function

```

was temporarily added to the model to simulate target metabolite production if the target metabolite did not have a production reaction.

The computational experiments focused on three key aspects: the success rate, the modification size, and the computation time. All the results were filtered by worst-case analysis, where only the minimum PR was evaluated under the GR maximization for each modification strategy. We used four different datasets from two major model species, *S. cerevisiae* and *E. coli*, downloaded from the BiGG database [12]. We constructed six datasets using these four datasets for the computational experiments for Prob-gDel and Prob-gDel-Add.

Table 1 represents the details of these six datasets. The iMM904 is a constraint-based model for *S. cerevisiae*, while both iJR904 and iML1515 are constraint-based models for *E. coli*. These three datasets were input for Prob-gDel, aiming to determine the deletion strategy. For Prob-gDel-Add, the edge model *E. coli* iJR904 was incorporated into the core model iMM904, while the edge model iND750 of *S. cerevisiae* was combined with the core models iJR904 and iML1515. The resulting integrated datasets exhibited an increase ranging from 300 to 400 in metabolites, 600 to 800 in reactions, and 500 to 600 in genes compared to their original counterparts. The efficacy of RatGene was benchmarked against gDel_minRN and GDLS using these six datasets. The allocated computational time for each target metabolite was limited to a specific threshold. All

fluxes with rates 10^{-3} or less were treated as having rates equivalent to zero.

Table 1. Datasets

ID	Dataset	Metabolites	Reactions	Genes
1	iMM904	1226	1577	905
2	iMM904+iJR904	1518	2186	1506
3	iJR904	761	1075	904
4	iJR904+iIND750	1139	1892	1419
5	iML1515	1877	2712	1516
6	iML1515+iIND750	2198	3560	2037

3.1 deletion-addition Problem: Prob-gDel-Add

Table 2 compares the performance of RatGene, gDel_minRN, and GDLS for Prob-gDel-Add on the three datasets. The row labeled ID 1 represents the number of metabolites whose theoretical maximum PR is more than 0.001. The rows labeled ID 2 to 4 represent the number of target metabolites for which each method could determine the modification strategy for growth-coupled production. The rows labeled ID 5 to 7 represent the success ratio. RatGene had the highest number of success and success rates on Datasets 4 and 6, where the success rate exceeded 26% on Dataset 4 and was nearly 40% on Dataset 6. gDel_minRN had the best performance for the number of successes and success rate on Dataset 2. The differences in success rates of RateGene and gDel_minRN are less than 5% for Datasets 2 and 4. The success ratio of RatGene was almost double that of gDel_minRN for Dataset 6. The success ratio of GDLS was much less than that of the best method across all datasets.

The rows labeled IDs 8 and 9 represent the size of the union and the intersection of the successful cases by RatGene and gDel_minRN. The rows labeled IDs 10 and 11 represent their percentages. If we executed both RatGene and gDel_minRN and adopted better solutions, the success rate exceeded 35%. The size of the union is almost two to three times the size of the intersection.

Table 3 represents the average sizes of additions and deletions in the modification strategies derived by the three methods. Rows labeled IDs 1 to 3 represent the size of deletions for each method and dataset, while rows labeled IDs 4 to 6 represent the size of additions. RatGene yielded smaller deletions compared to gDel_minRN for all three datasets. GDLS returned smaller average deletion sizes across all these datasets, but this result is less competitive when considering its low success rates. Regarding the addition sizes, RatGene consistently returned the smallest average sizes, all below 70. In contrast, the smallest average size for additions by gDel_minRN was 74.46. Although GDLS had the smallest average deletion sizes, it had much larger average addition sizes when compared to RatGene and gDel_minRN. For both RatGene and gDel_minRN, the average addition sizes were lower than the average deletion sizes for all datasets. In contrast, GDLS displayed the reverse results.

Table 4 displays the average computation time for each metabolite of all successful cases. RatGene had the lowest average computational time on Dataset 2, while GDLS

Table 2. Number of Success and Success Ratio(%)

ID	Dataset	iMM904+iJR904	iJR904+iND750	iML1515+iND750
		Dataset 2	Dataset 4	Dataset 6
1	TMPR > 10^{-3}	825	569	1295
2	RatGene	270	150	506
3	gDel_minRN	310	127	285
4	GDLS	61	79	33
5	RatGene(%)	32.73%	26.36%	39.07%
6	gDel_minRN(%)	37.58%	22.32%	22.01%
7	GDLS(%)	7.39%	13.88%	2.55%
8	^a Union	395	204	593
9	^b Intersection	185	73	198
10	Union(%)	47.88%	35.85%	45.79%
11	Intersection(%)	22.42%	12.83%	15.29%

^a The union results of RatGene and gDel_minRN.

^b The intersection results of RatGene and gDel_minRN.

Table 3. Average Modification Size

ID	Dataset	iMM904+iJR904	iJR904+iND750	iML1515+iND750
		Dataset 2	Dataset 4	Dataset 6
1	RatGene(^a Del)	553.19	608.91	1014.25
2	gDel_minRN(Del)	684.94	676.98	1127.15
3	GDLS(Del)	1.07	0.75	0
4	RatGene(^a Add)	67.13	31.24	50.89
5	gDel_minRN(Add)	168.74	74.46	88.14
6	GDLS(Add)	600.49	514.99	521.00

^a The size of deletions strategies.

^b The size of addition strategies.

was the fastest on the other two datasets. In computing the modification strategy in each dataset, the average computational time of RatGene for the successful cases was less than one-third to one-sixth of gDel_minRN. Based on the results of the success rates in Table 2, RatGene made fast computations while ensuring a relatively good performance in terms of success rates.

3.2 Deletion Problem: Prob-gDel

Table 5 compares the performance of RatGene, gDel_minRN, and GDLS for Problem 2 on the three datasets. Similar to Section 3.1, the row labeled ID 1 represents the number of metabolites whose theoretical maximum PR is more than 0.001. The rows labeled ID 2 to 4 represent the number of target metabolites for which each method could determine the modification strategy for growth-coupled production. The rows labeled ID 5 to 7 represent the success ratio. RatGene had the highest number of successes and success rates on Datasets 1 and 5, whereas gDel_minRN had the highest on Dataset 3. RatGene

Table 4. Average Computational Time of Successes (seconds)

Dataset	RatGene	gDel_minRN	GDLS
iMM904+iJR904 (Dataset 2)	162.83	541.06	197.66
iJR904+iND750 (Dataset 4)	180.37	547.18	33.45
iML1515+iND750 (Dataset 6)	85.36	585.66	20.39

Table 5. Number of Success and Success Ratio(%)

ID	Dataset	iMM904 Dataset 1	iJR904 Dataset 3	iML1515 Dataset 5
1	TMPR > 10^{-3}	782	510	1092
2	RatGene	210	38	262
3	gDel_minRN	172	224	211
4	GDLS	58	33	1
5	RatGene(%)	26.85%	7.45%	23.99%
6	gDel_minRN(%)	21.99%	43.92%	19.32%
7	GDLS(%)	7.42%	6.47%	0.09%
8	^a Union	296	236	386
9	^b Intersection	86	26	87
10	Union(%)	37.85%	46.27%	35.35%
11	Intersection(%)	11.00%	5.10%	7.97%

^a The union results of RatGene and gDel_minRN.

^b The intersection results of RatGene and gDel_minRN.

and GDLS had nearly identical low success rates on Dataset 3. GDLS exhibited a notably lower success rate and fewer successes compared to the other two methods across all datasets.

The union of successful results generated by RatGene and gDel_minRN promised to have the lowest success rate of over 35%. The intersection between RatGene and gDel_minRN only contributed a small amount, indicating that RatGene was efficient in obtaining successful deletion strategies that gDel_minRN could not find.

Table 6 represents the average sizes of deletion strategies derived by the three methods. RatGene produced successful deletion strategies with smaller average sizes than gDel_minRN for all three datasets. In contrast, the average strategy size of GDLS was fewer than ten across all these datasets. For both RatGene and gDel_minRN, the average deletion sizes for iMM904, iJR904, and iML1515 were lower than the results for the associated integrated datasets in Table 3. However, the average sizes for deletion strategies generated by GDLS on iMM904, iJR904, and iML1515 were either equal to or larger than those for their respective integrated datasets in Table 3.

Table 7 represents the average computation time for each metabolite of all the successes on Datasets 1, 3, and 5. GDLS had the lowest average computational time on the datasets, while the success ratio of GDLS is very low. The RatGene took less than 50% of the time to compute the deletion strategy on all three datasets compared to gDel_minRN. It was observed that RatGene computed much faster for the deletion-addition strategies in

Table 6. Average Deletion Size

Dataset	iMM904	iJR904	iML1515
	Dataset 1	Dataset 3	Dataset 5
RatGene	480.79	409.53	865.72
gDel_minRN	621.88	523.31	967.33
GDLS	6.53	2.52	0

Table 4 compared to the deletion strategies, while gDel_minRN took longer to compute on the integrated datasets than on its original datasets.

Table 7. Average Computational Time of Successes (seconds)

Dataset		RatGene	gDel_minRN	GDLS
iMM904	(Dataset 1)	248.39	532.24	134.46
iJR904	(Dataset 3)	241.77	520.68	43.22
iML1515	(Dataset 5)	259.26	570.28	3.72

4 Discussion and Conclusion

4.1 Discussion

Since the performance of RatGene and gDel_minRN was much better than GDLS, we focus on RatGene and gDel_minRN in the following discussion. RatGene solves Prob-gDel-Add by (1) integrating two constraint-based models and (2) determining gene deletion strategies for the integrated model. For solving Prob-gDel-Add, (2) of RatGene can be replaced with other algorithms such as gDel_minRN and GDLS because their purposes are the same. Tables 2 to 4 compare the performance of such three algorithms for Prob-gDel-Add. Similarly, Prob-gDel can be solved by gDel_minRN and GDLS, but (2) of RatGene also can solve it. Tables 5 to 7 compare the performance of the three algorithms for solving Prob-gDel.

Tables 2 and 5 show that RatGene and gDel_minRN exhibited strong performance for most datasets regarding both Prob-gDel-Add and Prob-gDel. While RatGene outperforms gDel_minRN for certain datasets, gDel_minRN is superior for others. Since the union of their successful cases was large and the intersection was small, RatGene and gDel_minRN can complement each other effectively. Therefore, by conducting both RatGene and gDel_minRN simultaneously, the performance can be significantly improved compared to using each individually.

Tables 3 and 6 display that RatGene derived smaller modification strategies than gDel_minRN. Table 3 indicates that the sizes of both deletions and additions of gDel_minRN were larger than those of RatGene. These differences came from the differences in the behavior of gDel_minRN and (2) of RatGene. Consequently, both RatGene and gDel_minRN can complementarily identify effective modification strategies for various target metabolites. The deletion sized by RatGene and gDel_minRN may further be reduced by the trial-and-error-based methods proposed in [27, 28].

Table 8. Increase in the number of success cases in the integrated models when compared to the original models

Dataset	iMM904+iJR904 Dataset 2	iJR904+iIND750 Dataset 4	iML1515+iIND750 Dataset 6
RatGene	60	112	244
gDel_minRN	138	-97	74
GDLS	3	46	32
TMPR > 10^{-3}	43	59	203

Tables 4 and 7 indicate that the computational speed of RatGene was more than three times faster than gDel_miRN in Prob-gDel-Add, and more than twice as fast in Prob-gDel. Therefore, running both RatGene and gDel_minRN simultaneously improved the success rate, but it also increased the computational time by more than threefold.

It is easier to find a growth-coupled production strategy in the integrated model created by N_1 and N_2 than in the model created by N_1 alone. Table 8 shows the increase in the number of growth-coupled production strategies identified by each method after the model integration when compared to the original models. The last row of Table 8 shows the number of target metabolites whose TMPRs were greater than zero in the integrated model but zero in the original model. On all data sets, the increase of target metabolites for which modification strategies were found by RatGene was larger than the increase of metabolites whose TMPRs were greater than zero. This means that RatGene successfully identified efficient modification strategies for many target metabolites for which strategies for growth-coupled production could not be obtained in the original dataset. Either RatGene or gDel_minRN exhibited an increase of more than 40 in the number of successful cases compared to the increase in the number of target metabolites with a TMPR > 10^{-3} for each dataset. For Dataset 4, the performance of gDel_minRN was not as good as in the original Dataset 3. This was due to the time limit set for each metabolite and the integrated models are larger than their original models. This indicates that RatGene is more efficient for large models than gDel_minRN.

Table 9. Average computational time by RatGene for all target metabolites with TMPR > 10^{-3} (seconds).

	iMM904	iJR904	iML1515
Prob-gDel	442.36	508.89	450.95
Prob-gDel-Add	223.31	245.04	136.53

Table 9 shows the average computational time taken by RatGene for all metabolites with TMPRs greater than zero. It shows that the average time for Prob-gDel was approximately 13% longer on dataset iJR904 compared to the other two datasets. The average time cost for Prob-gDel was more than double the average time cost for Prob-gDel-Add. These trends can be attributed to the reason that the computation continued until reaching the upper limit of calculation time when a solution was not found. RatGene primarily functions by iteratively assigning a fixed value to α to determine its value under growth-coupled production conditions. This process increases α from 0 to its

maximum within a predefined computation time limit. Consequently, the computation might be halted before identifying α if its appropriate value is relatively large. For deletion problems in the iJR904 model, the success rate of RatGene was initially 7.45% as shown in Table 5. This rate significantly increased to 26.36% after integrating the iND750 model, as shown in Table 2. The integration altered the network topology and the appropriate value of α , leading to a reduced average computation time of 245.04 seconds and an enhanced success rate as shown in Tables 9 and 2.

Figure 5 compares the average sizes of addition strategies before and after the size reduction. The average sizes of the strategies decreased to approximately 50%–65% of their original sizes. This demonstrates the effectiveness of the proposed process in compressing the size of the modification strategies.

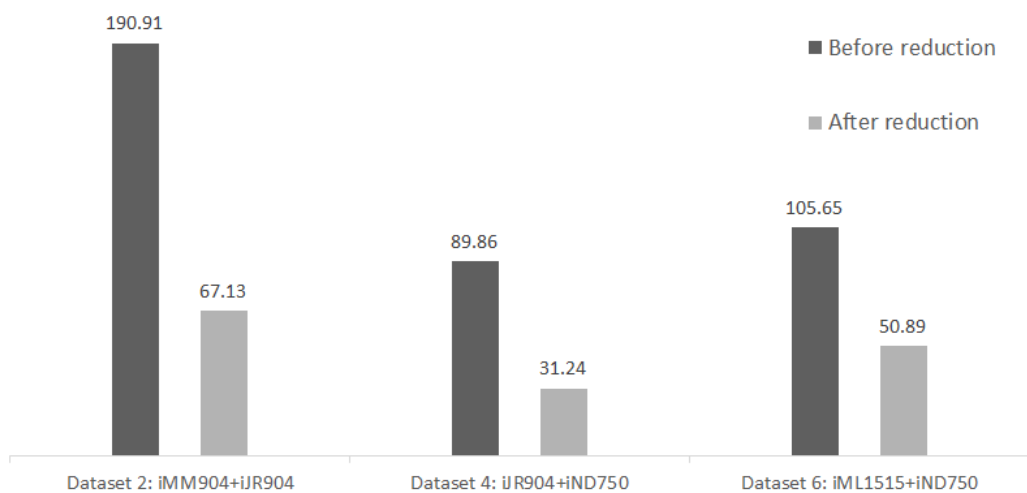


Figure 5. The average size of addition strategies before and after the size reduction.

4.2 Conclusion

In this study, we (1) mathematically defined Prob-gDel and Prob-gDel-Add, (2) proved their NP-completeness, and (3) developed RatGene. RatGene aims to solve Prob-gDel-Add by integrating two constraint-based models and identifying gene deletion strategies for growth-coupled production. RatGene can be used to solve Prob-gDel as well. The results of the computational experiments showed that RatGene is effective for solving Prob-gDel and Prob-gDel-Add, in particular for target metabolites for which the best existing methods cannot solve. By using gDel_minRN and RatGene in a complementary manner, the success ratios for Prob-gDel and Prob-gDel-Add can significantly be improved. RatGene identifies the strategies by growth-to-production ratio-based flux assignments. This improves the success ratio for identifying the strategies for growth-coupled production while it increases the computation time.

4.3 Related works

Numerous studies have been conducted on metabolic design for growth-coupled production. However, they mainly focus on reaction-level modifications, and did not appropriately consider GPR rules for genome-scale models. Existing methods can be roughly classified into elementary modes (EMs) and constraint programming-based methods.

The EM-based methods are briefly summarized below. The CASOP computational framework offers a strategy for strain optimization, using significance measurements of reactions derived from weighted EMs [3]. Approach based on Minimal cut sets (MCSs) combining a duality framework in metabolic networks was provided, where the task of counting the MCSs in the original network is simplified to determining the EMs in a dual network [1]. Constrained MCSs (cMCSs) -based method was proposed to systematically list all comparable gene deletion combinations, supporting the development of effective knockout strategies for coupled product and biomass production [4]. Effective preprocessing procedures have been described to be utilized by algorithms that computes cMCSs from EMs, and it was shown how computing MCSs from EMs could be made comparable by a modest adjustment to the integer program [5]. MCSEnumerator merged two methods to offer the MCS enumerator, which was a novel technique for efficiently enumerating the smallest MCSs by determining shortest EMs in genome-scale metabolic network models with the fewest interventions [30]. An approach that focused on how to meaningfully assess and order a set of computed metabolic engineering strategies for growth-coupled product synthesis has also been proposed [20]. Another work categorized different growth-coupled productions into four groups and extended the MCS framework to calculate the strain designs using the implicit optimality constraints [21].

Constraint programming-based methods are briefly summarized below. A bilevel programming framework called Optknock was made available for locating knockout strategies [2]. Various methods based on this bilevel optimization have been proposed subsequently [15, 17, 18]. FastPros offers a unique screening technique in which the potential of a given reaction knockout for the synthesis of a particular metabolite is assessed by the shadow pricing of the constraint in the flux balance analysis [13]. GridProd is a grid-based optimization method framework that separates the entire constraint space of the problem into grids and searches for potential deletion strategies in the subspaces [24]. minL1-FMDL, a fast metabolic design listing algorithm, was developed to provide narrowed reaction deletion strategies in polynomial time [26]. Based on this framework, several methods have been proposed to explore the design of metabolic networks under different environmental conditions [8, 25].

Data Availability

The developed scripts are available on <https://github.com/Ma-Yier/RatGene>.

References

1. K. Ballerstein, A. von Kamp, S. Klamt, and U.-U. Haus. Minimal cut sets in a metabolic network are elementary modes in a dual network. *Bioinformatics*, 28(3):381–387, 2011.
2. A. P. Burgard, P. Pharkya, and C. D. Maranas. Optknock: a bilevel programming framework for identifying gene knockout strategies for microbial strain optimization. *Biotechnology and bioengineering*, 84(6):647–657, 2003.
3. O. Hädicke and S. Klamt. Casop: a computational approach for strain optimization aiming at high productivity. *Journal of biotechnology*, 147(2):88–101, 2010.
4. O. Hädicke and S. Klamt. Computing complex metabolic intervention strategies using constrained minimal cut sets. *Metabolic engineering*, 13(2):204–213, 2011.
5. C. Jungreuthmayer, G. Nair, S. Klamt, and J. Zanghellini. Comparison and improvement of algorithms for computing minimal cut sets. *BMC bioinformatics*, 14(1):1–12, 2013.
6. S. Y. Lee and H. U. Kim. Systems strategies for developing industrial microbial strains. *Nature biotechnology*, 33(10):1061, 2015.
7. D. S. Lun, G. Rockwell, N. J. Guido, M. Baym, J. A. Kelner, B. Berger, J. E. Galagan, and G. M. Church. Large-scale identification of genetic design strategies using local search. *molecular systems biology*, 5(1):296, 2009.
8. Y. Ma and T. Tamura. Dynamic solution space division-based methods for calculating reaction deletion strategies for constraint-based metabolic networks for substance production: Dyncubeprod. *Frontiers in Bioinformatics*, 1:716112, 2021.
9. D. Machado, M. J. Herrgård, and I. Rocha. Stoichiometric representation of gene–protein–reaction associations leverages constraint-based analysis from reaction to gene-level phenotype prediction. *PLoS computational biology*, 12(10):e1005140, 2016.
10. C. D. Maranas and A. R. Zomorodi. *Optimization methods in metabolic networks*. John Wiley & Sons, 2016.
11. J. Nielsen and J. D. Keasling. Engineering cellular metabolism. *Cell*, 164(6):1185–1197, 2016.
12. C. J. Norsigian, N. Pusarla, J. L. McConn, J. T. Yurkovich, A. Dräger, B. O. Palsson, and Z. King. Bigg models 2020: multi-strain genome-scale models and expansion across the phylogenetic tree. *Nucleic acids research*, 48(D1):D402–D406, 2020.

13. S. Ohno, H. Shimizu, and C. Furusawa. Fastpros: screening of reaction knockout strategies for metabolic engineering. *Bioinformatics*, 30(7):981–987, 2014.
14. J. D. Orth, I. Thiele, and B. Ø. Palsson. What is flux balance analysis? *Nature biotechnology*, 28(3):245–248, 2010.
15. K. R. Patil, I. Rocha, J. Förster, and J. Nielsen. Evolutionary programming as a platform for in silico metabolic engineering. *BMC bioinformatics*, 6(1):308, 2005.
16. P. P. Peralta-Yahya, F. Zhang, S. B. Del Cardayre, and J. D. Keasling. Microbial engineering for the production of advanced biofuels. *Nature*, 488(7411):320–328, 2012.
17. P. Pharkya, A. P. Burgard, and C. D. Maranas. Optstrain: a computational framework for redesign of microbial production systems. *Genome research*, 14(11):2367–2376, 2004.
18. S. Ranganathan, P. F. Suthers, and C. D. Maranas. Optforce: an optimization procedure for identifying all genetic manipulations leading to targeted overproductions. *PLoS Comput Biol*, 6(4):e1000744, 2010.
19. Z. Razaghi-Moghadam and Z. Nikoloski. Genereg: A constraint-based approach for design of feasible metabolic engineering strategies at the gene level. *Bioinformatics*, 2020.
20. P. Schneider and S. Klamt. Characterizing and ranking computed metabolic engineering strategies. *Bioinformatics*, 35(17):3063–3072, 2019.
21. P. Schneider, R. Mahadevan, and S. Klamt. Systematizing the different notions of growth-coupled product synthesis and a single framework for computing corresponding strain designs. *Biotechnology Journal*, 16(12):2100236, 2021.
22. S. Schuster and C. Hilgetag. On elementary flux modes in biochemical reaction systems at steady state. *Journal of Biological Systems*, 2(02):165–182, 1994.
23. M. Sipser. Introduction to the theory of computation. *ACM Sigact News*, 27(1):27–29, 1996.
24. T. Tamura. Grid-based computational methods for the design of constraint-based parsimonious chemical reaction networks to simulate metabolite production: Gridprod. *BMC bioinformatics*, 19(1):325, 2018.
25. T. Tamura. Efficient reaction deletion algorithms for redesign of constraint-based metabolic networks for metabolite production with weak coupling. *IPSI Transactions on Bioinformatics*, 14:12–21, 2021.

26. T. Tamura. L1 norm minimal mode-based methods for listing reaction network designs for metabolite production. *IEICE TRANSACTIONS on Information and Systems*, 104(5):679–687, 2021.
27. T. Tamura. Trimming gene deletion strategies for growth-coupled production in constraint-based metabolic networks: Trimngdel. *IEEE/ACM Transactions on Computational Biology and Bioinformatics*, 2022.
28. T. Tamura. Metnetcomp: Database for minimal and maximal gene-deletion strategies for growth-coupled production of genome-scale metabolic networks. *IEEE/ACM Transactions on Computational Biology and Bioinformatics*, 2023.
29. T. Tamura, A. Muto-Fujita, Y. Tohsato, and T. Kosaka. Gene deletion algorithms for minimum reaction network design by mixed-integer linear programming for metabolite production in constraint-based models: gdel_minrn. *Journal of Computational Biology*, 2023.
30. A. von Kamp and S. Klamt. Enumeration of smallest intervention strategies in genome-scale metabolic networks. *PLoS computational biology*, 10(1):e1003378, 2014.
31. A. von Kamp and S. Klamt. Growth-coupled overproduction is feasible for almost all metabolites in five major production organisms. *Nature communications*, 8:15956, 2017.